

Article

# Noise Impact Assessment of UAS Operation in Urbanised Areas: Field Measurements and a Simulation

Filip Škultéty \* , Erik Bujna, Michal Janovec  and Branislav Kandra

Faculty of Operation and Economics of Transport and Communications, University of Žilina, Univerzitná 8215/1, SK-010-26 Žilina, Slovakia

\* Correspondence: filip.skultety@uniza.sk

**Abstract:** This article's main topic is an assessment of unmanned aircraft system (UAS) noise pollution in several weight categories according to Regulation (EU) 2019/947 and its impact on the urban environment during regular operation. The necessity of solving the given problem is caused by an increasing occurrence of UASs in airspace and the prospect of introducing unmanned aircraft into broader commercial operations. This work aims to provide an overview of noise measurements of two UAS weight categories under natural atmospheric conditions to assess their impact on the surrounding environment. On top of that, modelling and simulations were used to observe and assess the noise emission characteristics. The quantitative results contain an assessment of the given noise restrictions based on the psychoacoustic impact and actual measured values inserted into the urban simulation scenario of the Zilina case study located in northwest Slovakia. It was preceded by a study of noise levels in certain areas to evaluate the variation level after UAS integration into the corresponding airspace. Following a model simulation of the C2 category, it was concluded that there was a marginal rise in the level of noise exposure, which would not exceed the prescribed standards of the Environmental Noise Directive.



**Citation:** Škultéty, F.; Bujna, E.; Janovec, M.; Kandra, B. Noise Impact Assessment of UAS Operation in Urbanised Areas: Field Measurements and a Simulation. *Drones* **2023**, *7*, 314. <https://doi.org/10.3390/drones7050314>

Academic Editors: Andrzej Łukaszewicz, Wojciech Giernacki, Zbigniew Kulesza, Jaroslaw Alexander Pytka and Andriy Holovatyy

Received: 21 March 2023

Revised: 2 May 2023

Accepted: 3 May 2023

Published: 9 May 2023



**Copyright:** © 2023 by the authors. Licensee MDPI, Basel, Switzerland. This article is an open access article distributed under the terms and conditions of the Creative Commons Attribution (CC BY) license (<https://creativecommons.org/licenses/by/4.0/>).

**Keywords:** drone; UAS noise measurement; noise emission characteristics; noise modelling; noise simulation; Zilina case study

## 1. Introduction

In the near future, the concept of parcel and medicine delivery by drones, increasingly associated especially with the perceptions of global shipping carriers, is a challenge for many research areas. It is expected that there will be an enormous increase in the number of unmanned aerial vehicles (UAVs) used not only for commercial operations but also for recreational purposes. With increased unmanned aircraft system (UAS) traffic, there is also a presumption of increased noise in the surrounding environment and the adverse impact of psychoacoustic phenomena on humans or animals.

The significance of this work lies in assessing the characteristics of the noise spreading by multirotor drones regarding the risks of psychological influences and negative impact on the population. The intention is to create a background for the future investigation of regular UAS operations through the practical introduction of the case study via a simulation environment. At present, there is no uniform rule for measuring and assessing the noise of drones, and each Member State has its regulations for this purpose, which are mostly based on a uniform ISO standard. Therefore, our future work will contain the assessment of whether actual legislation is adequate and whether there will be a necessity to implement new harmonised rules for EU member states.

The noise assessment was based on previous measurements and results used in our measurements and assumptions in determining the characteristics of sound spreading in space. These measurements were preceded by studies and examinations of the UAV noise sources and the influence of the external environment, which had to be considered

in other contexts. It is necessary to focus on a specific location when assessing noise, even when putting unmanned vehicles into operation. A study of legislation, current restrictions, and impacts on humans and wildlife preceded it. Based on information on legislation and measurements of sound propagation in the environment, it is possible to assess the effects on humans and provide data for further research and model situations in the natural environment.

### 1.1. Theory of Sound and Rotor Noise

The production of sound is achieved through the transmission of vibrations that propagate through the layers of air. This process involves the disturbance of air particles, which can be visualised as sinusoidal waves with varying amplitudes that correspond to the intensity of the sound. The peaks of the sinusoidal waves occur when the air particles are compressed and subsequently expanded.

#### 1.1.1. Equations

The gap between the repeating wave period of sound waves is wavelength  $\lambda$  (m), tightly connected with the frequency of the sound  $f$  (Hz) and speed of sound  $c$  ( $\text{m}\cdot\text{s}^{-1}$ ), which is the speed of spreading of acoustical waves in air. It depends on actual atmospheric conditions with the most significant influence on temperature [1].

$$\lambda = c/f \quad (1)$$

The sound can be transferred from the source, which could be a monopole, dipole, or quadrupole. This statement forms the basis of the theory of sound developed by Lord Rayleigh in the nineteenth century [2].

The sound source emits the tones with some power. This is called sound power, with the unit watt (W). This energy is transmitted through the air per unit of time. The air serves as a surface through which the sound is transferred, which is the sound intensity with the unit ( $\text{W}/\text{m}^2$ ). Since the sound intensity is a relation between sound power and the surface of wave propagation whose sound is transported, the equation is:

$$I = W/S \quad (2)$$

Moreover, when the sound is transferred in every direction, it is possible to write the equation for sound power:

$$W = 4\pi r^2 I \quad (3)$$

where  $r$  is the radius in a sphere (m); during observation, this is one of the minor variables of sound pressure. During measurement, microphones do it all the time. This pressure is responsible for the displacement of air molecules in all directions [1]. The relation between sounds we hear with exact power and the reference power is called the sound power level,  $L_W$ . It is measured in decibels and could be expressed via logarithmic function [2]. The reference power is considered to be 10–12 W. This is because it represents the lowest sound humans may discern. This parameter is used to measure overall noise regardless of the location because sound power level is not a function of distance from the sound source.

$$L_W = 10\log W/W_{\text{ref}} \quad (4)$$

In the same way, as shown in Equation (4), it is possible to identify sound intensity levels where sound power  $W$  and reference power  $W_{\text{ref}}$  are replaced by sound intensity  $I$  ( $\text{W}/\text{m}^2$ ) and reference sound intensity  $I_{\text{ref}}$ . Sound intensity is a parameter showing the direction and amount of acoustic energy in a specific area. However, sound pressure level (SPL)  $L_p$  is used to identify how loud the source of sound is. It is the difference between a sound wave and the ambient pressure the sound travels through. Before expressing the

equation for SPL, it is necessary to mention that it is feasible to express sound intensity in Equation (1)

$$I = p^2 / \rho c \quad (5)$$

where  $p^2$  is the root mean square pressure (RMS),  $\rho$  is the density of air ( $\text{kg}\cdot\text{m}^{-3}$ ), and  $c$  is the speed of sound ( $\text{m}\cdot\text{s}^{-1}$ ). Additionally, the RMS pressure is used in the equation for SPL, which is proportional to the PWL equation and can be expressed as “ten times logarithm to the base 10 of the square of sound pressure  $p$ , to the square of a reference value  $p_{\text{ref}}$ , expressed in decibels” [3]

$$L_p = 10 \log p^2 / p_{\text{ref}}^2 \quad (6)$$

$$L_p = 20 \log p / p_{\text{ref}} \quad (7)$$

Reference values for both sound intensity and sound power are known. Reference sound intensity was set as  $I_{\text{ref}}$  equals 10–12 W/m and reference sound power was set as  $W_{\text{ref}}$  equals 10–12 W. In a numerical way, intensity and sound pressure levels are almost equal in room temperature and sea level pressure. When the area of the surface is taken into account, sound pressure level and sound power level are related to each other as:

$$L_p = L_W - 10 \log S \quad (8)$$

where  $S$  is the surface through which sound is transported. From this relation,  $P_{\text{ref}}$  is taken as equivalent with sound power but, generally, it is known as the limit of audibility, 20 ( $\mu\text{Pa}$ ).

The last variable that it is important to incorporate during the measurement process is the distance of the source of the sound from the receiver. Distance has to be included when the sound of the exact source is measured due to the inverse square law [4].

### 1.1.2. Rotational Propeller Noise

Noise radiating from the rotor consists of three components: blade slap, rotational noise, and vortex noise. In the case of rotors, it is caused by a lack of symmetry. The advancing blade meets air with higher velocities during a forward flight than the retreating blade. Another essential feature of the rotor aerodynamic is the rotor wake from a noise and vibration point of view. Amplitudes of higher harmonics specific to helicopters or UAVs vary and also depend on flight conditions. A large part of the detectable noise observed is related to vortex effects.

External inputs also affect every numerical calculation, which limits the accuracy of calculations. However, blade slap noise is more complex for hand calculations and more sophisticated software is necessary for its calculations. Assumptions made by M.V. Lowson, which help to analyse and calculate trends of the behaviour of rotational noise generated by rotors during steady flight, can be used to achieve and use reasonable and valuable results of noise harmonics, which differ from computer calculations by no more than 2 dB [1].

## 1.2. Literature Review

Literature synthesis contributes to developing new insights and perspectives and helps identify gaps or inconsistencies in the previous research. In the databases, it is possible to reveal a trend and the frequency of the occurrence of scientific works on similar topics. Leslie, Wong, and Auld were among the first to focus on noise from UAS operations. They published a 2008 conference paper on broadband propeller noise reduction [5]. Massey and Gaeta dealt with noise measurements of tactical UAVs in 2010 [6]. Similar research was carried out in 2013 by Sinibaldi and Marino, particularly focused on experimental analysis of the noise of propellers for small UAVs [7]. The investigation involved generating an acoustic signature profile of a small multirotor UAS conducted by Kloet, Watkins, and Clothier [8]. Acoustic measurements carried out in an anechoic room were performed by Papa et al. as part of the research for a conference paper in 2016 [9].

We can include a computational study on the aeroacoustics of a multirotor unmanned aerial system by Heydari, Sadat, and Singh [10], and a combined experimental and numerical assessment of UAV noise emissions by Cussen, Garruccio and Kennedy [11] among the latest works that prove the relevance of the issue. Several works are also devoted, for instance, to noise certifications, such as [12], or preliminary research on transverse noise topics [13–21]. Nevertheless, there are only a few works conducted on real measurements according to official regulations on the noise of rotorcraft, followed by acoustic maps or simulation of noise propagation in a natural environment, which is the area of our interest. For example, Treichel et al. [22] conducted in 2022 a series of eight UAV noise measurements according to ISO standard 3744. However, the authors did not visualise the noise maps or directional characteristics of frequency analysis. On the other hand, Kenedy, Garruccio and Cussen [23] investigated the suitability of the software package ‘iNoise’ for modelling noise emission by drones. Relatively recent activity in the area of investigating the UAS impact as part of the U-space system is addressed by Deliverable D4.2 of DACUS Project [24]. The project has recognised the necessity of consolidating the concept of a social impact hotspot, which refers to a specific area where the demand for drone traffic results in noise and visual exposure that exceeds acceptable thresholds for a predetermined duration or frequency within a given period.

## 2. Materials and Methods

When the measurements were conducted, it was necessary to comply with specific conditions. Results of measurement might be affected by factors that cause them to deviate from results measured in an ideal reference area with specific reference conditions. These reference conditions are given and must be in compliance with approval by the certifying authority. Measurement in compliance with the reference procedure should follow reference atmospheric conditions:

- Sea level atmospheric pressure of 1013.25 hPa;
- Ambient temperature of 20 °C (ISA may be used);
- Relative humidity of 65%;
- Zero wind.

If the maximum rotor speed is given, the maximum operating rotor speed shall be taken as the highest speed, tolerance should be given on this speed, and measurement shall be conducted using this rotor speed. In case the rotor speed is adjustable maximum operating rotor speed for the reference conditions shall be used for the purpose of measurement and certification [25]. Test criteria, especially in case the measurement is in a non-airport area, should include criteria affecting results such as terrain, residual sound, weather conditions, microphone placement, and pilot sight [6]. Irregularities in terrain, such as mounds and furrows, can result in reflections and these surface anomalies may influence measured sound levels. Not only the terrain surface but also the highness of vegetation may influence the reflection of sound waves from ground level. Vegetation can result in the variation of sound level, more frequently with decreasing sound level, but the sound level may be higher. The surface of the measured area is also important, and the hardness of the surface is an important factor because hard surfaces, such as paved areas, may result in higher measured sound levels than soft ones.

Obstructions, for example, buildings, trees, vehicles, and even test personnel, may cause reflections that influence noise levels. For this reason, obstructions of this character are unacceptable in the vicinity of the measuring point. During measurement, there should not be any obstacle causing reflection in a conical shape area above the measurement device. Figure 1, created according to the ICAO standards [25], depicts this conical shape area defined as the axis normal to the ground and the axis formed by the angle of 80° around the vertical axis. Besides material, the object’s width is important in reflection consideration and environmental correction can be negligible.

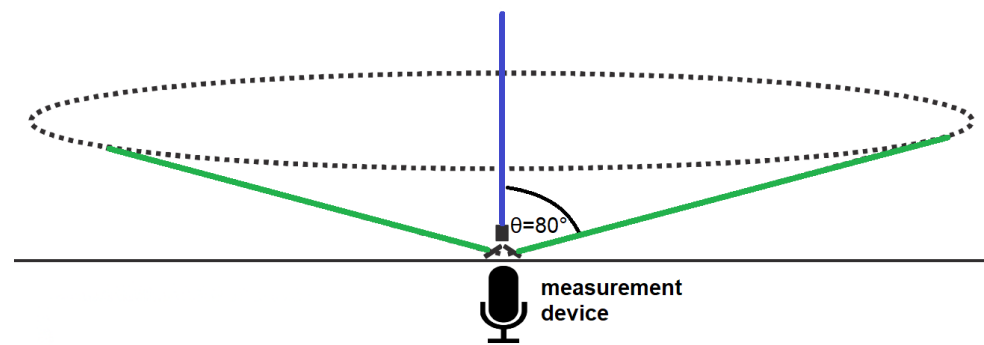


**Figure 1.** Conical area without obstructions during measurement.

### 2.1. Measurement Devices

For our experiment, NORSONIC Nor-140 measuring devices were used. Every chosen device is a hand-held device. They are composed of a microphone cartridge, microphone preamplifier, display, keyboard, sockets, and battery compartment. Our measurements were important mapping levels versus time display and level versus frequency. The display is possible to set as a dual view to observe more parameters at the same time. Nor-140 can also measure in the 120 dB range for one or one-third of an octave band. Every one of these three sound level meters is a measuring device class 1. It is possible to make a frequency analysis using the range within measuring devices depending on octave bands. The octave band has a wider span range than the third-octave bands. Nor-140 measures the range for frequency analysis in the one-third octave band from 0.4 Hz to 20 kHz. These span ranges are satisfactory for our experiment due to measuring frequencies which are hearable for the human ear. Basic measurement parameters are SPL,  $L_{Max}$ ,  $L_{Min}$ ,  $L_{Leq}$ , and  $L_{peak}$ . Results from measurements can be easily scanned through captured recordings in a measurement device without transferring data to a PC. However, it is more convenient to use a PC afterwards and post-process data in reporting software [26–28].

These data, which are measured in decibels referenced to 20  $\mu\text{Pa}$ , are updated at least once per second. In the settings, if necessary, it is always possible to switch measurements to another weighting. It is crucial because sound level meters respond differently to different sound frequencies compared with human hearing sensitivity. The most usable weighting is A because it measures the noise similarly, as humans are sensitive to sound. A-weighting is common for almost all environmental noise measurements. The analysis software may assess the result of equivalent sound-level data. Method, which is suitable for assessing noise audibility of tones, uses 1/3 octave measurements. One-third octave bands provide a more precise outlook on noise levels regarding frequency composition.

### 2.2. Evaluated UAVs

In our experiment, two types of drones were chosen, each representing a specific weight category. For each weight there are specified rules of flight determined in Regulation (EU) 2019/947. DJI Mavic 2 Pro and DJI Inspire 2 quadcopters were chosen for the experiment. The aforementioned regulation outlines the specific conditions under which the selected UAVs may be operated. Both are classified under the A2 sub-category of the ‘open’ category, which obtains the primary framework for most recreational drones and low-risk commercial operations. The elementary specifications of UAVs used in this evaluation are shown in Table 1. Size, weight and velocity data were obtained from the official store [29].

**Table 1.** Basic specifications of UAVs.

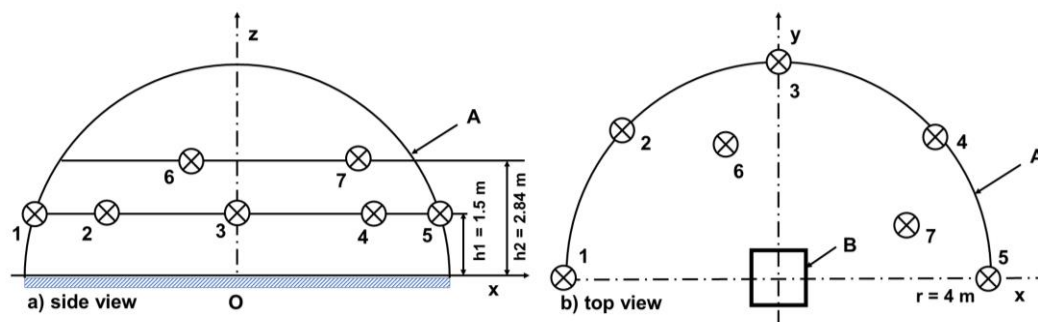
	DJI Mavic 2 Pro	DJI Inspire 2
Take-off weight (g)	907	3440
Dimensions with unfolded propellers (mm)	322 × 242 × 84	605 × 605 × 300
Max speed (km/h)	72	108
Weight category	C1	C2

### 2.3. Methodology

The methodology of outdoor measurements of UAS is described in the Commission delegated regulation (EU) 2020/1058 from 27 April 2020. This regulation should ensure the same conditions for measurement and it is based on ISO 3744 2010, where general conditions of measurement are described and methods of counting sound power levels are described. Part 13 describes the noise measurement prescription, which describes the determination of the A-weighted sound pressure level in the area surrounding the source of the sound.

The A-weighted time-averaged sound pressure level is measured at least three times for UAV configuration. Suppose a couple of these three measurements differ from the results by 1 dB. Measurements are repeated. The acoustic sound pressure level is the arithmetic mean of the two highest results. DJI Mavic 2 Pro belongs to category C1, whereas DJI Inspire, whose weight is 3440 g, belongs to category C2.

According to the Annex to Delegated Regulation (EU) 2019/945—Part 13 “The measurement surface shall have its origin at the point O lying in the ground plane directly below the UA”. The minimum flight and hovering height above ground level of selected DJI UAVs is 0.5 m. Therefore, the UAVs shall hover above a hard acoustic surface at a sufficient distance from any reflecting wall or ceiling, or any reflecting object so that the requirements given in Annex A of EN ISO 3744:2010 will be satisfied on the measurement surface. The measurement surface is the hemisphere with one origin point O, in the middle, shown in Figure 2. This figure shows the displacement of microphones during measurements. The displacement was managed according to Annex F of ISO 3744 2010 standard, where A determines the measurement surface, B determines the reference surface, and r determines the measurement surface radius which is 4 m.

**Figure 2.** Microphone array on a hemispherical measurement surface for measurement.

According to the Commission delegated regulation (EU) 2020/1058 from 27 April 2020, the measurement of A-weighted sound power level  $L_{WA}$  shall be executed above a hard surface with minimal sound absorption. This provides objective results compared to sound pressure measurements. It allows for determining the acoustic power emitted by the device regardless of the direction of noise from the source. Knowing the sound power level is very useful and it allows the sound output of different devices to be objectively compared.

For this reason, the former local airstrip mainly used for agricultural works in Rosina village was chosen, as shown in Figure 3. Fields surrounded the place where the measurement was executed and the highest possible permanent source of the sound, the highway, was distanced 3 km from the measuring place. Measurements were partially interrupted

by non-permanent sources of sound, e.g., passenger cars. In these times, measurements were paused and results were not included with these non-desirable factors.



**Figure 3.** Microphone array at the airstrip.

The placement of the microphones is displayed according to ISO 3744 2010 Annex F in Figure 3. According to regulations, microphones are needed for measurement purposes at positions 2, 4, 6, 8, 10, and 12. However, our measurement was a round base divided by two with microphones in positions 6, 8, 12. Turning the UAV and flying with UAVs back and forth created perception from both sides of UAVs and made the imaginary hemispherical area. The  $x$ -axis served as an overflight line with a hard pad in the middle of the axis and the centre of the thought circle served as starting pad during hovering measurements. Microphones 6 and 8 were deployed according to ISO 3744 2010 Annex F conditions in the  $x$ - and  $y$ -axis from the circle's centre point. These two were distanced from the  $x$ - and  $y$ -axis 2.62 m. These two microphones were placed at 1.5 m height AGL. The third microphone was distanced from the  $x$ -axis 2.6 m and from the  $y$ -axis 1.08 m. Its height deployment was 2.84 m AGL. This placement was used to measure equivalent sound pressure level  $L_{Aeq}$  and count sound power levels  $L_{WA}$  of each UAV.

The values of the A-weighted sound power levels, the sound power levels in the third-octave bands, and the A-level sound exposure level were measured with sound level meter strings based on Nor-140 sound analysers. NORSONIC N1225 measuring microphones with NORSONIC Nor1209 measuring preamplifiers were used to record audio signals. A total of three measurement strings were used to measure acoustic performance, four to measure flights, and sound exposure levels A were determined. The microphones were equipped with wind and dust covers with a diameter of 60 mm. The monitored quantities were determined based on measuring the time course of the values of short-term A-weighted equivalent sound pressure levels and equivalent sound pressure levels on third-octave bands with mean frequencies in the range of 20 Hz to 20 kHz. The averaging period was  $T = 125$  ms. The particular periods were continuously linked to each other during the time intervals of measurement of the respective flight operations, overflights, and hovering.

The determination of the value of the quantity describing the residual sound, the background noise, was determined from the values of the measured quantities at time intervals when no overflights were performed.

Verification of the correct sensitivity setting of the measurement strings was performed before and after all series of measurements were performed. Verification was performed using a reference signal source (microphone calibrator) NORSONIC Nor1251.

Sound analysers and specified elements of measuring chains, at the time of measurement, had valid verifications in accordance with the Act of the National Council of the Slovak Republic No. 157/2018 Coll. on metrology and related regulations, as amended.

#### 2.4. Calibration

When measuring the level of the assessed source and the noise of the assessed source, there is background noise, which is included in the total SPL level. If the difference between the total level and the background noise level is in the range from 3 dB to 18 dB, then the noise level of the assessed source is determined by level  $L_{Aeq}$  which is deducted by the correction  $K_1$  determined according to the equation:

$$K_1 = -10 \log(1 - 10^{-0,1(L_S - L_B)}) \quad (9)$$

where  $L_S$  means time-averaged sound pressure level, with source gained from the array of microphones in the measurement surface, and  $L_B$  means SPL of the background noise. If the difference exceeds 18 dB, the background noise negligibly affects the source level under consideration. The assessed value is then measured (resp. determined and adjusted for the length of exposure to noise sources), and the value of the determining quantity is increased by the measurement uncertainty adjusted by corrections and determined for the relevant reference time interval. Then:

$$L_{R,Aeq} = (L_{Aeq} + K_1 + K_T) \quad (10)$$

where  $L_{R,Aeq}$  is the assessed equivalent sound level A for the reference time interval,  $L_{Aeq}$  is equivalent sound level A for the reference time interval,  $K_1$  is the correction factor for background noise, and  $K_T$  is the assessed value for specific noise determined by adding the correction  $K_T = +5$  dB to the equivalent sound level A unless otherwise stated. The day and evening  $K_T$  correction only applies if the total duration of the specific noise exceeds 10 min per day or 5 min per evening.

When 50 dB residual sound was recorded during measurements, the difference in Figure 4 illustrates the adjustment between the residual sound and the sound from the source in the 20 to 25 dB range. This means that the correction for  $K_1$  is negligible and, after substituting the values into Equation (9), the correction for  $K_1$  is up to 0.1 dB.

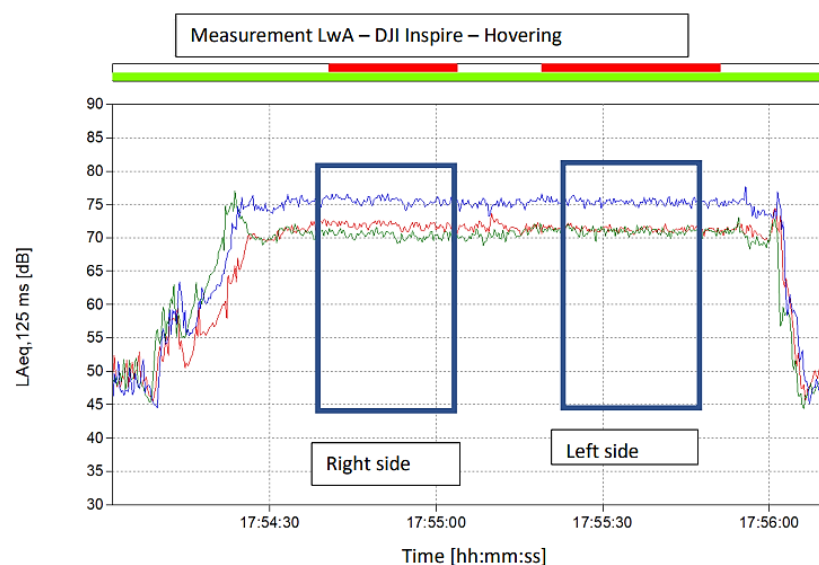


**Figure 4.** Equivalent sound pressure levels in time of DJI Inspire during hovering.



### 3. Results

Figures 4 and 5 describe  $L_{Aeq}$  during hovering and overflight of the DJI Inspire from UAV weight category C2, which provide an illustrative view of the perception of microphones during two flight modes. As mentioned, the microphones were placed on half the measuring surface. Therefore, the measurements were performed twice with the UAV rotated in both directions. The rotation of the UAV concerning the microphones is shown in both figures by dark blue rectangles. Each side was measured with three microphones. Therefore, for both figures, the record on the right contains microphones M2 marked in red, M6 marked in blue, and M4 marked in green, and the record on the left contains microphones M1 marked in green, M7 marked in blue, and M3 marked in red colour. In this way, the entire surface needed to perform the measurements was covered.

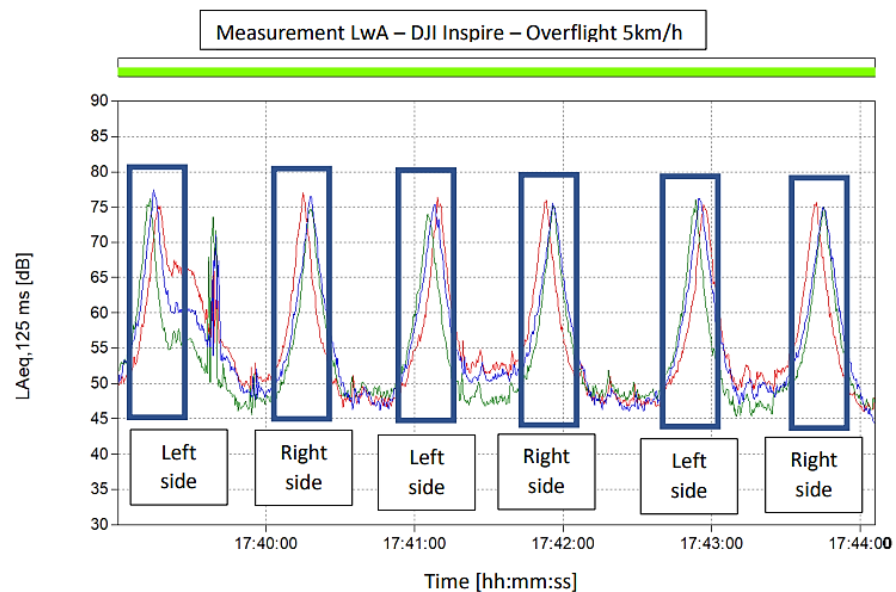


**Figure 5.** Equivalent sound pressure levels in time of DJI Inspire during the overflight.

From Figure 4, it is possible to observe the value of the residual sound before the UAV takes off over a solid surface of 0.5 m. From the graph, it is possible to find that the microphones at positions 6 and 7 recorded a higher level of  $L_{Aeq}$  than the four microphones distributed along the edges of the area at a lower height. This value differs from the values measured on four microphones while hovering by approximately 5 dB.

In Figure 5 are expressed the results of six DJI Inspire overflights at a speed of 5 km/h. The depicted  $L_{Aeq}$  noise levels present three flyovers in each direction along the specified section of the asphalt runway. In the time period between 17:39 and 17:40 you can spot the discrepancy in the measurement, which was caused by passage of the motorcycle on the road located right next to the airfield.

Measurements when UAVs were hovering above the hard surface and overflying the measuring area were performed for weight categories C1 and C2 with their representatives DJI Mavic 2 Pro and DJI Inspire 2. Measurements evaluated the A-weighted equivalent sound pressure level  $L_{Aeq}$ . However, in order to compare the noise load for comparison between chosen weight categories, it is necessary to convert the averaged equivalent sound pressure levels to sound power levels  $L_{WA}$ , using Equation (11), where  $S$  is the area of the measurement surface and  $S_0$  equals  $1 \text{ m}^2$ . Results for DJI Inspire are displayed in Table 2 and for DJI Mavic 2 Pro in Table 3. These results compare the  $L_{WA}$  of UAVs from the C1 category, mostly used in the hobby sphere, and C2, which might also be used in commercial operations, from both categories; this is described as maximal  $L_{WA}$  in the Commission delegated regulation (EU) 2020/1058.

$$L_{WA} = L_{Aeq} + 10 \log S/S_0 \quad (11)$$

**Table 2.** Corrected equivalent sound pressure levels of DJI Inspire 2.

Middle Filter Frequency (Hz)	Acoustic Sound Power Level Corrected with $L_{WA}$ Equation (dB)			
	5 kmh <sup>-1</sup>	10 kmh <sup>-1</sup>	20 kmh <sup>-1</sup>	Hovering
20	13.9	6.4	9.3	11.2
40	24.9	23.6	22.0	22.5
80	40.3	40.7	44.1	36.9
160	65.1	65.5	71.9	56.2
315	75.6	76.4	80.2	63.1
630	78.2	81.8	81.7	69.2
1250	83.0	83.9	85.3	73.1
2500	83.5	83.8	85.6	72.7
5000	79.9	82.6	84.4	69.5
10,000	71.6	75.3	77.3	62.5
20,000	58.8	64.2	67.6	51.3

**Table 3.** Corrected equivalent sound pressure levels of DJI Mavic 2 Pro.

Middle Filter Frequency (Hz)	Acoustic Sound Power Level Corrected with $L_{WA}$ Equation (dB)			
	5 kmh <sup>-1</sup>	10 kmh <sup>-1</sup>	20 kmh <sup>-1</sup>	Hovering
20	8.4	8.2	13.2	14.7
40	21.4	20.2	24.8	36.3
80	33.9	38.0	39.3	40.3
160	53.0	57.6	63.9	53.3
315	64.1	66.4	67.8	60.9
630	66.5	70.2	73.7	67.0
1250	70.0	73.6	76.1	70.7
2500	68.6	72.4	75.1	70.0
5000	67.8	70.3	73.7	68.9
10,000	65.0	65.5	67.7	64.7
20,000	55.8	54.5	55.8	54.2

Both Tables 2 and 3 show the A-weighted sound power levels during overflights at the height of 0.5 m, which is intended for measurements for this purpose of two drones at different speeds, as well as the values measured at 0.5 m above the ground during hovering. The measured values of  $L_{WA}$  are displayed in the range of the audible spectrum of the human ear from 20 Hz to 20 kHz.

Figures 6 and 7 depict a comparison of two drones, DJI Inspire 2 and DJI Mavic 2 Pro, during hovering and during overflight at a speed of 10 km/h. It is possible to see from a comparison of the graphs that, during hovering, the values of both categories are approximately the same when it is possible to observe similar levels of acoustic power at the same frequencies. However, as can be seen from Figure 6 at 10 km/h overflights, the DJI Inspire has been shown to reach higher  $L_{WA}$  than the DJI Mavic 2 Pro. However, during flights with DJI Mavic 2 Pro, higher frequencies were recorded at the same  $L_{WA}$ , which was audible with listening as “buzzing”, which may have the effect of annoyance of people around. The following case study focuses on the DJI Inspire 2 only.

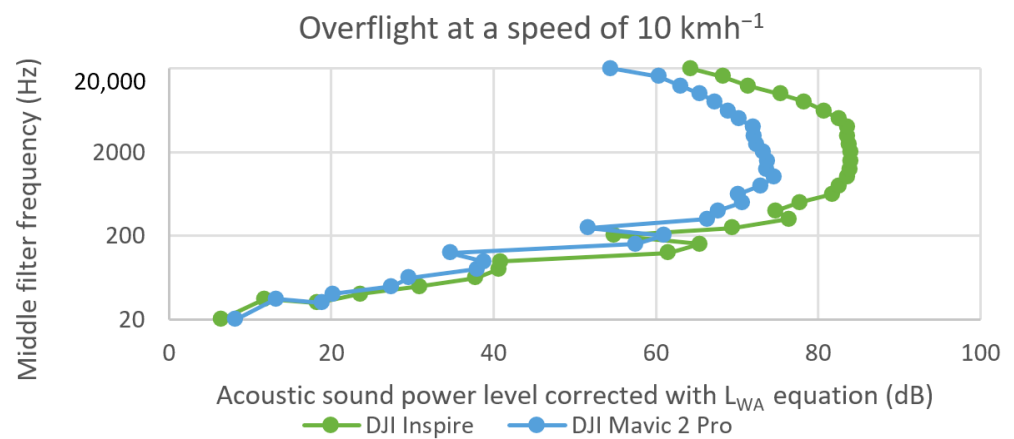


**Figure 6.** Comparison of  $L_{WA}$  for the two drones during overflight at a speed of  $10 \text{ kmh}^{-1}$  at 0.5 m height.

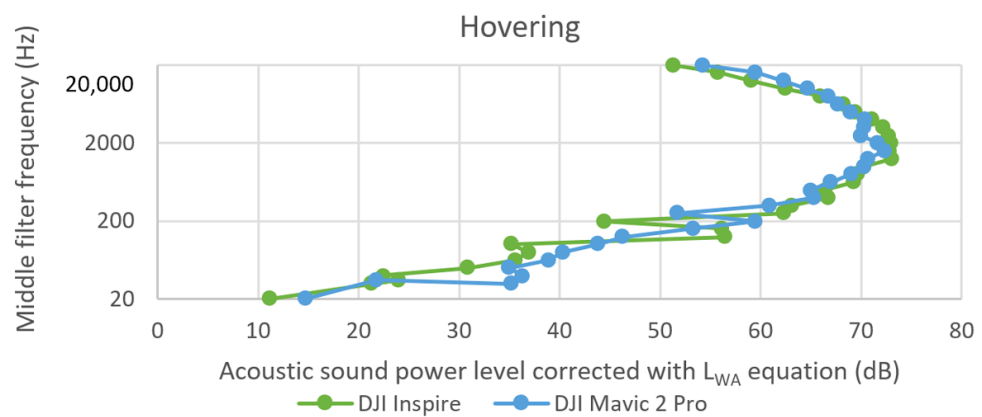


**Figure 7.** Comparison of  $L_{WA}$  for the two drones during hovering at 0.5 m height.

#### Simulation for Zilina Case Study

Based on the results, the implementation of the DJI Inspire 2 operation of weight category C2, which has the prerequisites to carry smaller goods, was considered according to cooperation with Mr. Kamenický [30]. The operation was intentionally simulated in the noise-sensitive environment of the University Hospital in Zilina. During this simulation, it was considered that DJI Inspire 2 might be able to transfer medication or blood from two pre-designated areas of the Faculty Hospital with the Polyclinic of Zilina.

The operation was simulated so that the UAV takes off from a place near the regional public health office building to a height of 50 m, the minimum height for flights over non-participants. According to the marked blue route, it will fly to the place near the building of the faculty hospital at the prescribed height and end its flight there.

The model situation was designed so that the UAV operation with one drone, DJI Inspire, with a speed of  $20 \text{ kmh}^{-1}$ , took place during the day reference time interval (12 h), defined from 6:00 to 18:00 with an average of 10 flights per hour with a total of 120 flights per day. The flight distance in this case study was 640 m. The duration of one UAV flight in the simulation was 120 s, excluding take-off and landing time.

For the visualisation of the case study, DataKustik GmbH CadnaA software was used. We started with the simulation of light rotorcraft (Robinson R22 Beta helicopter) noise propagation, which was modified according to our previously measured parameters. The aircraft database was based on the Integrated Noise Model (INM 7.0d), which is also recommended for noise mapping in the vicinity of airports. The ECAC Doc. 29 and AzB 2008 standards were alternatively considered. The noise model for the DJI Inspire 2 was modified and subsequently simulated for its flight path, taking into account the effects of atmospheric conditions and ground reflection. Both 2D and 3D visualisations were developed by the PlotDesigner function combined with the Eurosence Digital Terrain Model, including buildings and road corridors in the investigated geographical area.

Figures 8 and 9 graphically express the noise load of the selected place of operation, at a height of 1.5 m above the ground, which can be considered the ears' level. The difference between the two visualisations is as follows. The 2D visualisation contains a simulation of sound propagation in the given corridor. Figure 8 does not include residual sound, so it is possible to see that the noise load in the given area of the flight reaches the equivalent level of A-weighted sound from 40 to 45 dB. Due to the fact that the flight altitude is 50 m, the noise load at higher buildings in the area may be higher. The 3D visualisation (Figure 9) represents the resulting state of the investigated environment regarding road traffic noise, which was obtained based on the long-term measurements of the Euroakustik Ltd. Company, (Bratislava, Slovakia).

Since the noise load must be assessed based on the category of the specific area and the reference time interval, for this model situation, the operation in the first category of the territory with special noise protection during the day reference time interval is shown in which the maximum  $L_{Aeq}$  from other sources is defined by the Decree of the Ministry of Health of the Slovak Republic 549/2007 by 45 dB.

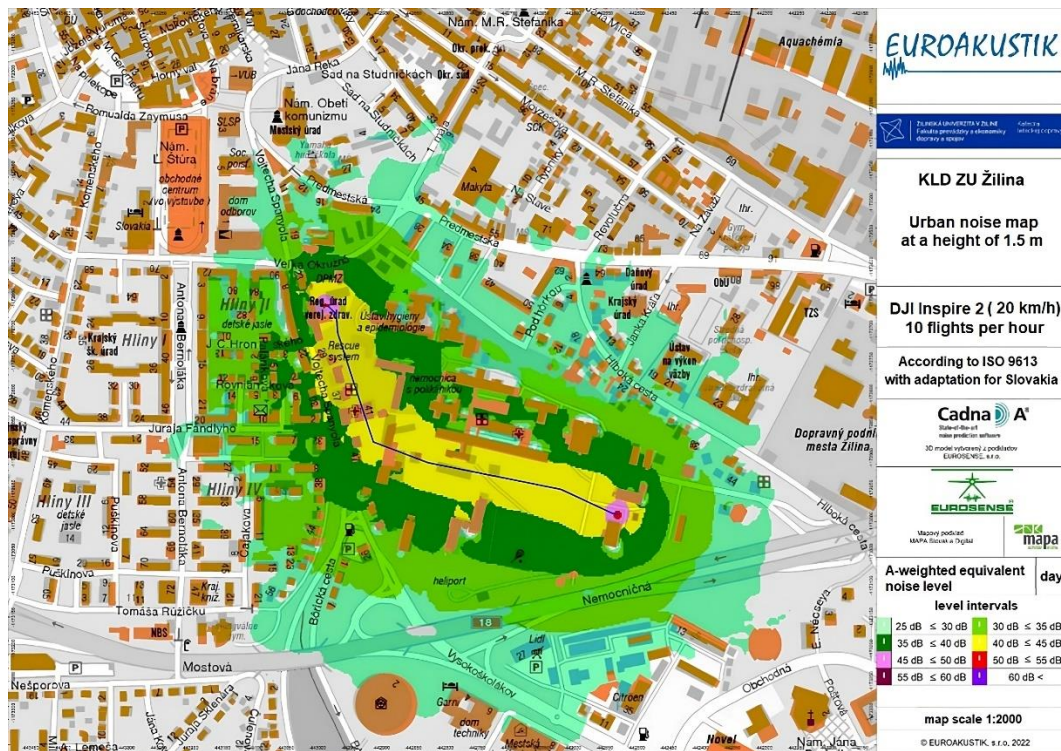


Figure 8. Noise load around flight corridor at 2D visualisation.



**Figure 9.** Noise load around flight corridor at 3D visualisation.

Concerning residual noise, it is necessary to assess the impact of whether the noise load of the examined sound source exceeds the noise load of surrounding objects such as roads. The impact of road noise was assessed in a 3D visualisation model situation in which it was found that the possible introduction of the UAV DJI Inspire 2 operation into the selected environment does not contribute to increasing the noise load.

From the model situation as well as the measured values, it is also possible to say that the commissioning of UAV DJI Inspire 2 will in no way cause health problems for people in the specific area and its short flight time over non-participants, which lasts only a few seconds, will not cause any long-term medical consequences associated with migraine headache or other problems.

#### 4. Conclusions

This work confirmed the source of sound sources radiated by drones, which can be encountered in the hobby and commercial spheres. The precondition for the creation of the manuscript was the vision that, in the future, drones could, in increased numbers, affect people's mental health and annoyance. In this work, we confirmed the parameters of sound propagation of drones in the environment that have been estimated or known so far. Following the evaluation of frequency analyses from indoor measurements were outdoor measurements, which were not affected by excessive ambient sound undesirable to detect the noise load. These measurements were performed to determine and compare UAVs' sound power levels during hovering and overflights at increased RPM corresponding to the operation. Based on the provided data, the  $L_{WA}$  of UAVs from the C1 and C2 categories were evaluated. The corrected equivalent sound pressure levels of DJI Inspire 2 and DJI Mavic 2 Pro were measured at different speeds and frequencies. At a middle filter frequency of 160 Hz, the  $L_{WA}$  of the DJI Inspire 2 ranges from 65.1 dB to 71.9 dB, while the  $L_{WA}$  of the DJI Mavic 2 Pro ranges from 53.0 dB to 63.9 dB, indicating that the Mavic 2 Pro produces less noise than the Inspire 2 at this frequency.

Based on the measured values, we found that UAVs used for hobby flying do not exceed the limits listed in the category of other sources in the decree of the Ministry of Health of the Slovak Republic. Also, after a model simulation in the specific area of the

commissioning of the UAV DJI Inspire, no significant increase in the noise load on the population was found.

In this work, the data were provided for implementing measurements and subsequent assessment of the impact of noise on the external environment in introducing unmanned aerial vehicles into actual operation. Based on spectral analyses, a graphic model of sound propagation from an unmanned aerial vehicle could be designed in the future and, with an assessment of its radiation characteristics, placed in the map base of a specific model situation from which the consequences for broad-spectrum use would be derived.

**Author Contributions:** Introduction F.Š. and E.B.; literature review F.Š., M.J., and B.K.; materials and methods E.B. and F.Š.; data curation F.Š. and B.K.; results F.Š., E.B., and B.K.; writing—original draft F.Š., E.B., and M.J.; visualisation M.J. and F.Š.; internal review and editing B.K. All authors have read and agreed to the published version of the manuscript.

**Funding:** This publication was realized with the support of Operational Program Integrated Infrastructure 2014–2020 of the project: Intelligent operating and processing systems for UAVs, code ITMS 313011V422, co-financed by the European Regional Development Fund.

**Institutional Review Board Statement:** Not applicable.

**Informed Consent Statement:** Not applicable.

**Data Availability Statement:** The article includes the original contributions presented in the study. Further inquiries can be directed to the corresponding author.

**Conflicts of Interest:** The authors declare no conflict of interest.

## Abbreviations

### Abbreviations

AGL	Above ground level
EU	European Union
ISA	International standard atmosphere
ISO	International Organization for Standardization
PC	Computer
PWL	Sound power level
RMS	Root mean square
RPM	Revolutions per minute
SPL	Sound pressure level
UAS	Unmanned aircraft system
UAV	Unmanned aerial vehicle

### List of symbols

$\lambda$	Wavelength
$f$	Frequency
Hz	Hertz
$c$	Phase velocity
dB	Decibel
W	Watt
m	Meter
Pa	Pascal
$P_{rms}$	Root mean square pressure
$\rho$	Density
$L_{Aeq}$	A-weighted equivalent continuous sound level
$L_{WA}$	A-weighted sound power level
$L_W$	Sound power level
$L_p$	Sound pressure level

## References

1. Marte, J.E.A.; Kurtz, D.W. *A Review of Aerodynamic Noise from Propellers, Rotors, and Lift Fans*, 1st ed.; NASA: Pasadena, CA, USA, 1970; pp. 11–47.
2. Sound\_Theory: Acoustics. Available online: <https://acoustics.no/sound-measurement/sound-theory> (accessed on 9 January 2023).
3. ISO 3744:2010; Acoustics—Determination of Sound Power Levels and Sound Energy Levels of Noise Sources Using Sound Pressure—Engineering Methods for an Essentially Free Field over a Reflecting Plane. ISO: Geneva, Switzerland, 2015. Available online: <https://www.iso.org/standard/52055.html> (accessed on 9 January 2023).
4. Longhurst, R.S. *Geometrical and Physical Optics*; Wiley: New York, NY, USA, 1967.
5. Leslie, A.; Wong, K.C.; Auld, D. Broadband noise reduction on a mini-UAV propeller. In Proceedings of the 14th AIAA/CEAS Aeroacoustics Conference (29th AIAA Aeroacoustics Conference), Vancouver, BC, Canada, 5–7 May 2008.
6. Massey, K.; Gaeta, R. Noise measurements of tactical UAVs. In Proceedings of the 16th AIAA/CEAS Aeroacoustics Conference, Stockholm, Sweden, 7–9 June 2010.
7. Sinibaldi, G.; Marino, L. Experimental analysis on the noise of propellers for small UAV. *Appl. Acoust.* **2013**, *74*, 79–88. [CrossRef]
8. Kloet, N.; Watkins, S.; Clothier, R. Acoustic signature measurement of small multi-rotor Unmanned Aircraft Systems. *Int. J. Micro Air Veh.* **2017**, *9*, 3–14. [CrossRef]
9. Papa, U.; Del Core, G.; Giordano, G. Determination of sound power levels of a small UAS during flight operations. In Proceedings of the 45th International Congress and Exposition on Noise Control Engineering (INTER-NOISE): Towards a Quieter Future, Hamburg, Germany, 21–24 August 2016; pp. 216–226.
10. Heydari, M.; Sadat, H.; Singh, R. A computational study on the aeroacoustics of a multi-rotor unmanned aerial system. *Appl. Sci.* **2021**, *11*, 9732. [CrossRef]
11. Cussen, K.; Garruccio, S.; Kennedy, J. UAV noise emission—A combined experimental and numerical assessment. *Acoustics* **2022**, *4*, 297–312. [CrossRef]
12. Senzig, D.A.; Marsan, M. UAS Noise Certification. In Proceedings of the Inter-Noise 2018 Impact of Noise Control Engineering Conference, Chicago, IL, USA, 6–29 August 2018.
13. Siljak, H.; Kennedy, J.; Byrne, S.; Einicke, K. Noise mitigation of UAV operations through a complex networks approach. In Proceedings of the INTER-NOISE and NOISE-CON Congress and Conference Proceedings, Glasgow, Scotland, 21–24 August 2022.
14. Roger, M.; Moreau, S. Tonal-noise assessment of quadrotor-type UAV using source-mode expansions. *Acoustics* **2020**, *2*, 674–690. [CrossRef]
15. Kim, D.H.; Park, C.H.; Moon, Y.J. Aerodynamic analyses on the steady and unsteady loading-noise sources of drone propellers. *Int. J. Aeronaut. Space Sci.* **2019**, *20*, 611–619. [CrossRef]
16. Schäffer, B.; Pieren, R.; Heutschi, K.; Wunderli, J.M.; Becker, S. Drone noise emission characteristics and noise effects on humans—A systematic review. *Int. J. Environ. Res. Public Health* **2021**, *18*, 5940. [CrossRef] [PubMed]
17. Park, C.H.; Kim, D.H.; Moon, Y.J. Computational study on the steady loading noise of drone propellers: Noise source modeling with the lattice Boltzmann method. *Int. J. Aeronaut. Space Sci.* **2019**, *20*, 858–869. [CrossRef]
18. Roy, M. Evaluation of Environmental Noise in urban areas: A noise pollution assessment approach. *Med. Agric. Environ. Sci.* **2022**, *2*, 21–40. [CrossRef]
19. Ramos-Romero, C.; Green, N.; Roberts, S.; Clark, C.; Torija, A.J. Requirements for drone operations to minimise community noise impact. *Int. J. Environ. Res. Public Health* **2022**, *19*, 9299. [CrossRef] [PubMed]
20. Alkmim, M.; Cardenuto, J.; Tengan, E.; Dietzen, T.; Van Waterschoot, T.; Cuenca, J.; De Ryck, L.; Desmet, W. Drone noise directivity and psychoacoustic evaluation using a hemispherical microphone array. *J. Acoust. Soc. Am.* **2022**, *152*, 2735–2745. [CrossRef] [PubMed]
21. Bian, H.; Tan, Q.; Zhong, S.; Zhang, X. Assessment of UAM and drone noise impact on the environment based on virtual flights. *Aerosp. Sci. Technol.* **2021**, *118*, 106996. [CrossRef]
22. Treichel, J.; Foerster, J.; Lieb, J.; Volkert, A. Anwendbarkeit der ISO 3744 Zur Ermittlung von Drohnengeräuschen/applicability of ISO standard 3744 for the determination of drone noise. *Lärmbekämpfung* **2023**, *18*, 50–54. [CrossRef]
23. Kennedy, J.; Garruccio, S.; Cussen, K. Modelling and mitigation of drone noise. *Vibroeng. Procedia* **2021**, *37*, 60–65. [CrossRef]
24. DACUS Research; Deliverable VALR D4.2: Brussels, Belgium. 2022. Available online: [https://dacus-research.eu/wp-content/uploads/2022/10/DACUS-VALR-D4.2\\_00.01.01-1.pdf](https://dacus-research.eu/wp-content/uploads/2022/10/DACUS-VALR-D4.2_00.01.01-1.pdf) (accessed on 15 April 2023).
25. ICAO. *Doc 9501 Environmental Technical Manual. Procedures for the Noise Certification of Aircraft*, 3rd ed.; ICAO: Montreal, QC, Canada, 2018; Volume 3.
26. Sound Analyser NOR118. Available online: <https://www.norsonic.asia/product/nor118> (accessed on 15 January 2023).
27. Sound Analyser NOR140. Available online: [https://web2.norsonic.com/product\\_single/soundanalyser-nor140](https://web2.norsonic.com/product_single/soundanalyser-nor140) (accessed on 15 January 2023).
28. Sound Level Meter-Analyser NOR145. Available online: [https://web2.norsonic.com/product\\_single/sound-level-meter-nor145](https://web2.norsonic.com/product_single/sound-level-meter-nor145) (accessed on 15 January 2023).

29. DJI Store—Official Store for DJI Drones, Gimbals and Accessories (Europe). Available online: <https://store.dji.com> (accessed on 15 January 2023).
30. Kamenický, M.; (Euroakustik Ltd, Bratislava, Slovakia); Bujna, E.; (University of Zilina). Personal communication, 2022.

**Disclaimer/Publisher’s Note:** The statements, opinions and data contained in all publications are solely those of the individual author(s) and contributor(s) and not of MDPI and/or the editor(s). MDPI and/or the editor(s) disclaim responsibility for any injury to people or property resulting from any ideas, methods, instructions or products referred to in the content.